

**Original Article**

DOI 10.1007/s12206-024-0143-8

**Keywords:**

- Parabolic collector
- Fresnel collector
- Solar energy
- Thermal analysis

**Correspondence to:**Cuma Çetiner  
cctiner@harran.edu.tr**Citation:**

Çetiner, C. (2024). Design, theoretical, and experimental thermal analysis of a solar collector with flat mirrors mounted on a parabolic surface. *Journal of Mechanical Science and Technology* 38 (2) (2024) 989–996.  
<http://doi.org/10.1007/s12206-024-0143-8>

Received August 15th, 2023

Revised October 6th, 2023

Accepted October 23rd, 2023

† Recommended by Editor  
Tong Seop Kim

# Design, theoretical, and experimental thermal analysis of a solar collector with flat mirrors mounted on a parabolic surface

**Cuma Çetiner**

Department of Mechanical Engineering, Faculty of Engineering, Harran University, Şanlıurfa, Turkey

**Abstract** Flat mirrors are used in Fresnel collectors. Mirrors arranged on the right and left reflect the sun's rays from a distance to the absorber. Meanwhile, parabolic transition-type collectors feature a reflective mirrored parabolic surface and are manufactured as a single unit. In this system, mirrors cut into 11 cm dimensions are placed on a parabolic surface. By incorporating flat mirrors onto the parabolic surface, a hybrid system combining parabolic and Fresnel collector types is created. The parabolic collector has an area of 15 m<sup>2</sup> with dimensions of 3.35 m × 4.5 m. This system tracks the sun in an east-west direction. Heat transfer oil is used as the heat transfer fluid of the system. In the experiment, the temperatures at the inlet and outlet, the glass tube in the absorber, and ambient temperatures were recorded. Theoretical thermal power and thermal efficiency results were compared with those obtained from experimental measurements. Findings indicate that the thermal efficiency of this system with a thermal power of 4 kW is around 30 %–39 %.

## 1. Introduction

Solar energy, as one of the renewable energy sources, has become an important energy source that can be freely harnessed without causing pollution. In the last decade, solar energy technology has attracted considerable attention due to its efficient and cost-effective production [1]. Parabolic trough collectors (PTCs) are widely used in various industries to achieve high temperatures using solar energy. Solar energy is increasingly employed for heating, cooling, and electricity generation. Solar concentrators play an important role in harnessing high temperatures from solar radiation [2]. PTCs are one of the most widely used technologies for converting solar energy into usable power because of their broad operating temperature range [3, 4]. These systems can achieve temperatures of 400–500 °C without requiring extensive parabolic surface areas [5–7]. In this technology, the sun's rays are focused on the absorber using reflectors. With parabolic solar collectors, the thermal energy collected in the absorber is transferred to a circulating heat transfer fluid (HTF) [8, 9]. Solar collectors are available in a variety of designs, typically classified into two categories: linear focus (Fresnel and parabolic collector types) and point focus (dish and tower types) [10, 11]. Parabolic collectors operate effectively with direct solar radiation and are particularly efficient in areas with abundant sunshine throughout the year.

Studies aimed at improving parabolic collectors, reducing their costs, and developing production technology are widespread. Begdouri [12] identified the 34 different PTC models available in the global solar market and summarized the key developments in the main PTC technologies, including exergy, exergy efficiency, and optical and thermal performance since the inception of the first PTC power plant. In a separate study, Kumar [13] comprehensively reviewed the evolution of DSG technology and the challenges in its commercialization. He experimentally and numerically investigated the sizing and design of the solar field, as well as the control system required to maintain the desired operating characteristics. Al-Rabeeh [14] discussed the

enhancement of thermal efficiency in the parabolic slotted solar collector system through the use of four different vacuum absorbers in the experiment: copper, single tube, ring, and double absorber tube. He presented the results of his experimental work. Uzair [15] performed a probabilistic modeling to establish the correlation between the HTF temperature obtained at the outlet of a linear parabolic collector. For this purpose, he developed a physical analytical model and compared the results with published values. In another study [16], Uzair claimed that the concentration ratio used in the parabolic slotted collector is valid only up to a certain receiver width. In cases where the receiver exceeds this width, the optical concentration ratio should be used. Ongoing research in this field includes efforts to improve parabolic collectors and enhance their thermal and optical performance [17, 18].

Among the solar concentrators used to harness solar energy, linear Fresnel collectors (LFCs) are an alternative to technologies like PTCs. These collectors are often chosen for their cost-effectiveness despite somewhat lower efficiency [19]. LFC-focused solar collector technology is an attractive option for supplying thermal energy to processes that require heat in the mid-temperature range and is widely used in various industrial applications [20]. LFCs concentrate solar radiation using a series of straight, long, and parallel mirrors. The rays reflected from these flat mirrors are transferred to a liquid circulating in the absorber located at the focal point of the system. The receiver at the focal point in Fresnel collectors can be a flat or composite absorber that reflects the radiation a second time [21, 22]. LFC arrays offer several advantages solar concentration due to their simplicity. The absorber construction for LFCs can be either single or double layered [maria]. Worldwide efforts have been made to achieve high temperatures using LFC technology, including the development of LFC prototypes, such as the one produced in Belgium by Solarmundo [23]. The Plataforma Solar de Almeria has worked on prototype projects to reach temperatures of 400 °C with LFCs in Spain and Italy. Noteworthy contributions to the development of linear Fresnel technology have been made by companies such as Novatec Solar, Areva Solar, and SkyFuel [24, 25]. Numerous studies have focused on improving the performance of LFC through using flat collectors and compound absorbers [26, 27]. The optical efficiency of LFC is lower than that of parabolic and dish collector types, primarily due to that not all reflected rays are perfectly focused on the absorber [28]. Nevertheless, focusing losses are less pronounced in parabolic corrugated collectors and dish-type collectors. In the study by Kincad, annual optical efficiency figures were reported as 60 % for the selected PTC, 52 % for the selected central receiver technology, and 40 % for the selected LFCs [29]. With regard to solar energy concentrators, thermal efficiency varies depending on the characteristics of the absorber and reflector. However, thermal efficiency is generally around 60 %–70 % [30, 31] for paraboloid bowl-type collectors, 45 %–50 % [32] for parabolic collectors, and 35 %–45 % [33, 34] for Fresnel and cylindrical collectors [35].

Numerous studies have explored the optics, thermal efficiency, production, and costs associated with parabolic collectors and LFCs. Ramasamy experimentally investigated a hybrid collector that combines features of PTC and LFC by using an optical ray tracing model on a parabolic LFC. Optical and thermal modeling revealed that high-performance LFC achieves an average optical efficiency of 49 % [36]. In a separate study, Morin compared the electricity generation costs between LFC and PTC. His findings suggested that the total cost of installing LFC systems could be approximately 20 % lower [37]. Maria investigated the losses due to shading and reflected rays reaching the absorber by characterizing the optical analysis of rays entering the mirror area of Fresnel collectors with hourly assumptions throughout the year [38].

In the case of parabolic collectors, the reflective mirror surface takes the form of a monolithic parabola. In this study, a parabolic surface was initially constructed using steel. Then, small flat mirrors were mounted on this parabolic surface. Unlike the single-piece parabolic mirror face used in some collectors, multiple flat mirrors were used, which resembles the configuration found in Fresnel collectors. The use of flat mirrors in this parabolic collector results in focusing losses in the absorber, which lead to lower thermal efficiency and optical efficiency than those for collectors with solid mirrors. However, due to the difficult of obtaining monolithic parabolic mirrors in the market, the use of this design is preferred for its ease of manufacture. In this collector with an area of 15 m<sup>2</sup>, the theoretical thermal power is estimated to be 5 kW, while the experimental thermal power is around 4 kW. The results show that the theoretical thermal efficiency is approximately 55 %, while the experimental thermal efficiency is nearly 40 %.

## 2. Material and method

### 2.1 Manufacturing and working principle of the parabolic collector

Considering factors such as the reflection rate of the reflector, the absorption rate of the absorber, transmittance density, and average regional radiation values, the dimensions of this parabolic collector were chosen to theoretically reach a thermal power of 5 kW. The parabolic collector measures 4500 mm in length and 3500 mm in width. It is equipped with a sun sensor, as shown in Fig. 1, which enables it to track the sun's movement in an east-west direction. The collector automatically adjusts its position using the electronic card in the control unit shown in Fig. 2 to respond to input from the sun sensor. Manual control allows the collector to be oriented east or west as needed. Incoming solar radiation is reflected from the PTC surface and concentrated on the absorber. An electric motor rotating at 900 rpm was selected to facilitate low-speed rotation of the system. Two gearboxes (Fig. 1), one with a ratio of 1/50 and the other with a ratio of 1/60, are connected to this electric motor to achieve lower rotational speed. In addition, a re-

Table 1. Lengths of the parabola in the x and y directions.

Y (cm)	20.94	41.88	62.81	83.75	104.69	125.63	146.56	167.5
X (cm)	1.19	4.75	10.69	19.0	29.69	42.75	58.19	76

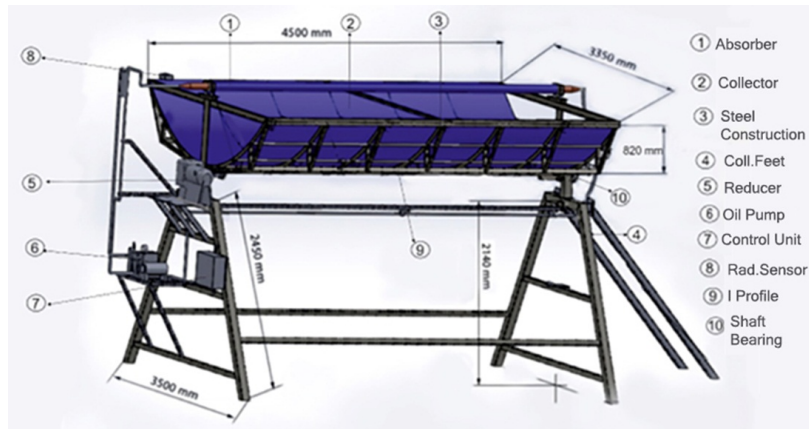


Fig. 1. Construction dimensions of the parabolic collector.



Fig. 2. Reflection of the sun's rays on the pipe at the focal point of the parabolic collector.

duction relay is used in the control unit to reduce the speed.

The fluid circulated in the system is HTF, which can withstand temperatures up to 325 °C, and it is driven by an oil pump. Data logger recorded the inlet and outlet temperatures of the HTF, the outer surface temperature of the glass tube, and the ambient temperature. The absorber size of the collector was intentionally chosen to be slightly larger than the collector size itself, considering the variation in the sun's rays between summer and winter. The copper pipe, which has a diameter of 76 mm, has a wall thickness of 2 mm. The inlet and outlet ends are tapered to allow 1/2 inch diameter connecting hoses. The absorber copper tube is situated in a glass tube with an outer diameter of 100 mm and a thickness of 2 mm. The head parts of the glass pipe are connected to the system with a specially manufactured metal construction, while the middle part is supported to protect it from vibrations [35].

The dimensions of the reflective parabolic collector surface are determined using Eq. (1). Flat mirrors were cut in 11 cm and mounted on this surface. Then, the theoretical thermal power and thermal efficiency results were compared with the thermal power and thermal efficiency obtained from the ex-

perimental measurements.

## 2.2 Calculations for collector manufacturing

The dimensions of the parabolic adder were determined from the parabola Eq. (1). The characteristic dimensions of the PTC are given in Table 1.

$$y = \sqrt{4fx} . \quad (1)$$

The parabolic aperture  $2y = 3.35$  m, with a height of  $x = 0.76$  m and a focal length  $f = 0.92$  m (Fig. 3).

As shown in Fig. 4, the plane mirrors in this collector are arranged tangent to the parabolic profile. The edges of the mirrors are aligned with the parabolic profile, as shown in Fig. 4. In this design, the small space that exists between the mirrors is an important factor in reduced collector performance. This gap can be minimized by smoothing the mirror edges.

## 2.3 Thermal analysis of the parabolic collector

While some of the radiation reaching the absorber from the concentrator is lost to the low-temperature environment, another portion is absorbed by the fluid and converted into useful energy. To calculate the useful energy transferred to the absorber in parabolic collectors, the thermal energy transferred to the fluid as described by the Hottel–Willer–Bliss equation can be used, as described below [39].

$$Q_u = A_a F_R \left[ I_a \alpha_p \gamma \tau - \frac{A_y}{A_a} U_T (T_m - T_a) \right] . \quad (2)$$

In this equation,  $Q_u$  is the useful heat energy,  $A_a$  is the aper-

Table 2. Characteristics of PTC.

Aperture of the collector	w	3350 mm
Length of the collector	L	4500 mm
Aperture area of the collector	Aa	15 m <sup>2</sup>
Depth of the collector	lp	760 mm
Focus of the parabola	f	920 mm
Concentration ratio	c	14
Rim angle	r <sub>rim</sub>	92°
Outer diameter of glass tube	dc	100 mm
Outer diameter of copper tube	db	76 mm

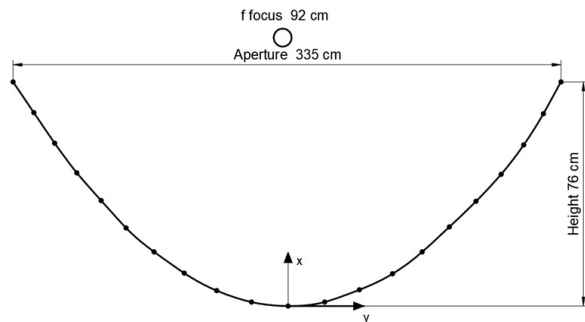


Fig. 3. Aperture, height, and focal distance of the parabola.

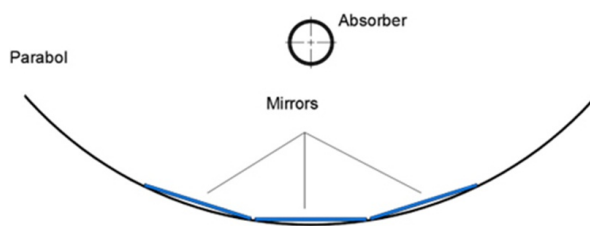


Fig. 4. Mirror edges aligned with the parabolic profile.

ture area,  $A_y$  is the absorber area,  $F_R$  is the heat gain factor, and  $(I_d)$  represents the amount of direct radiation falling on the unit aperture area.  $\alpha$  is the absorption rate of the absorber material,  $\gamma$  is the intercept factor,  $\rho$  is the reflectance rate of the reflective material, and  $\tau$  is the transmittance coefficient of the transparent cover.  $U_T$  is the total heat transfer coefficient from the absorber to the environment, and  $T_{in}$  is indicated by the fluid inlet temperature and the ambient temperature ( $T_a$ ).

The thermal efficiency of the concentrator and the useful thermal power of the collector are determined based on the aperture area of the parabolic collector and the rate of incident direct radiation. Accordingly, the theoretical thermal efficiency is calculated as follows [40]:

$$\eta_0 = \frac{Q_u}{A_a I_d} = F_R (\alpha \rho \tau) - F_R U_T \frac{A_y (T_{in} - T_a)}{A_a I_d} . \quad (3)$$

When the inlet and temperatures of the fluid and the experimental values such as the flow rate are known, the experimental thermal power can be calculated using the equation given

below:

$$Q = m c_p (T_{out} - T_{in}) . \quad (4)$$

Here,  $m$  is the mass flow rate (kg/sn), and  $T_{out}$  is the exit temperature of the fluid from the absorber. Thermal efficiency is defined as the ratio of the amount of HTF to the direct solar energy received by the total reflective surface. Accordingly, the experimental thermal efficiency is calculated as follows:

$$\eta = \frac{Q}{A_a I_d} . \quad (5)$$

### 3. Calculation of total heat transfer coefficient

For the heat gain and loss in the parabolic collector, the total heat transfer coefficient in the pipe must be calculated. The total heat transfer coefficient  $U_T$ , which includes conduction from the absorber to the environment, convection, radiation, and heat losses, can be determined using Eq. (6) below [40].

$$U_T = \left[ \frac{A_y}{A_a (h_{bc} + h_{rc})} + \frac{1}{h_w} \right]^{-1} . \quad (6)$$

Absorber losses occur due to radiation and convection emitted from the outer surface of the pipe to the environment. The radiation resistances in the pipe in terms of convection need to be calculated, as shown in the total heat transfer equation. Forced convection occurs on the outer surface of the glass tube due to ambient wind. Reynolds and Nusselt values need to be determined to meet the conditions of forced convection. A Nusselt value suitable for a horizontal glass pipe can be found in Ref. [41].

$$Nu = \frac{\rho V D_c}{\mu} = 0.25 Re^{0.6} Pr^{0.38} . \quad (7)$$

After obtaining  $Nu$  from the equation, the forced ( $h_{bc}$ ) value is determined.

The rate of heat transfer between surfaces due to radiation is influenced by the difference in surface temperatures raised to the fourth power. However, in many engineering applications, mathematical operations are performed to calculate the radiation exchange between the glass tube and the environment, as shown in the equation below [42].

$$h_{rc} = \epsilon_r \sigma (T_c + T_a) (T_c^2 + T_{cev}^2) . \quad (8)$$

The radiation coefficient between the copper tube and the glass tube is determined using Eq. (8), where  $T_c$  is the transparent cover temperature,  $\sigma$  is the Stefan-Boltzman constant,

and  $\epsilon_c$  is the radiation emission coefficient of the surface. The radiation between the copper tube and the glass tube is the radiation between two parallel plates and is calculated in terms of convection using Eq. (9) below.

$$h_w = \frac{\sigma(T_c + T_{cev})(T_c^2 + T_{cev}^2)}{\frac{1}{\epsilon_r} + \frac{A_r}{A_a} \left( \frac{1}{\epsilon_c} - 1 \right)} \quad (9)$$

From Eqs. (7)-(9) above, the total heat loss coefficient for the absorber is calculated by substituting Eq. (6).

The heat gain factor FR for the collector used in the useful power equation is found in the following Eq. (10).

$$F_R = \frac{\dot{m}c_p}{A_i U_T} \left[ 1 - \exp\left(-\frac{A_y U_T F}{\dot{m}c_p}\right) \right] \quad (10)$$

In this context, the collector efficiency factor F is not influenced by the operating conditions but rather depends on the design of the collector. This value can be calculated using the equation below.

$$F = \frac{1}{U_r} \left[ \frac{1}{U_T} + \frac{d_d}{h_w d_i} + \frac{d_d \ln\left(\frac{d_d}{d_i}\right)}{2k} \right] \quad (11)$$

When the values in Eqs. (10) and (11) are placed in their respective positions, the heat gain factor FR is determined to be 0.98.

## 4. Results and discussion

The experiments for this parabolic collector were conducted in Şanlıurfa ( $e = 37.1^\circ$ ) between 8 am and 5 pm. HTF was circulated at a low flow rate in this collector, which had dimensions of  $3.35 \times 4.5$  m. The primary goal was to improve the thermal performance of the PTC by enhancing the thermal efficiency of the thermal receiver, which is a critical element in a PTC system. The thermal performance of PTCs can be improved through working on the internal structure and materials of the absorber. Alam et al. summarized key findings from the literature on conventional or nanofluidic HTFs by reviewing studies aimed at increasing efficiency in PTC absorbers [43]. By using Eq. (6) given above for the absorber used in the experiment, the total heat transfer coefficient from the glass pipe to the environment was calculated to be around  $10.4 \text{ W/m}^2 \text{ }^\circ\text{C}$ . Given that the copper pipe lacked a selective surface, an absorption rate of 0.82, a transmittance coefficient of 0.88 for the glass pipe, and a relatively low reflectivity (0.82) were chosen for the reflective surface given that it was not a mirrored surface. An intersection factor of 0.95 was chosen due to frag-

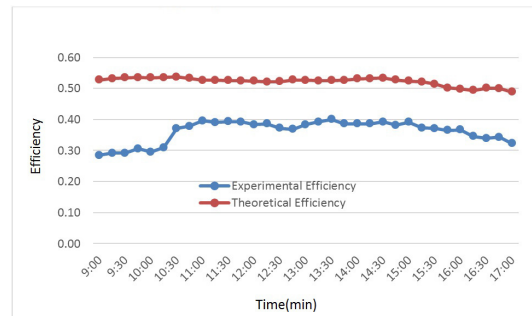


Fig. 5. Theoretical and experimental thermal efficiency.

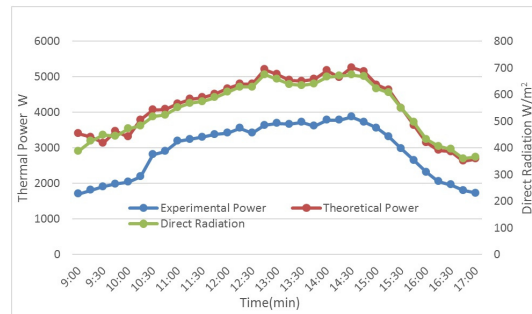


Fig. 6. Theoretical and experimental thermal power and direct radiation values.

mented nature of the reflective surface [44]. With these values, the theoretical thermal efficiency value was calculated to be around 54 %–58 % (Fig. 6). The experimental efficiency was determined using Eq. (5), which relied on the HTF inlet and outlet temperatures and flow rates from the experiment. Fig. 5 shows that the curve depicting the experimental efficiency closely aligns with the theoretical thermal efficiency in the afternoon. Based on the calculations using experimental data, the thermal efficiency ranged from 30 % to 39 %. Satpute found the thermal efficiency to be around 35 %–39 % for a parabolic collector [45].

The measured direct radiation value is around  $400\text{--}700 \text{ W/m}^2$ , which was obtained from the radiation measurement center at Harran University's Engineering Faculty. The experimental set was set up at a distance of 30 m from this measurement center. Theoretically, the parabolic collector (Fig. 7) can generate approximately 5200 W of thermal power. The selected values for reflection rate, transmittance, and absorption coefficient in the theoretical calculation are effective. The experimental values closely align with the expected useful power value at noon. However, due to lower solar radiation intensity in the morning and evening, the thermal power values decrease accordingly. Calculations based on experimental values indicate that the experimental thermal power varies between 2000 and 3900 W (Fig. 6).

Although the glass pipe temperature varies slightly in the experimental measurements in the collector, a noticeable alignment is observed among the ambient, glass pipe, and HTF inlet and outlet temperatures (Fig. 7). Considering the relatively

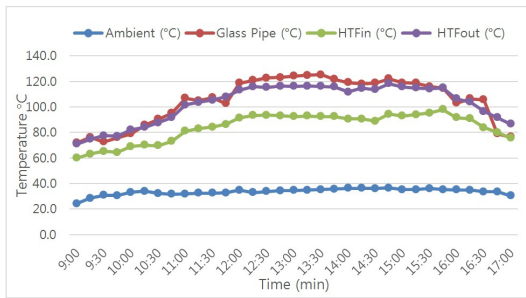


Fig. 7. Ambient, glass pipe, and HTF inlet and outlet temperatures measured in the parabolic collector.

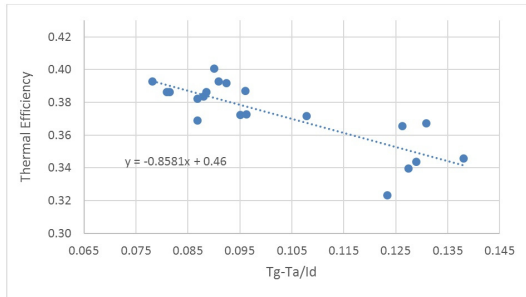


Fig. 8. Thermal efficiency of the collector for hot HTF.

small size of the parabolic collector, the difference between the HTF inlet and outlet temperatures remains minimal.

Fig. 8 shows the graph obtained by dividing the thermal data by the direct radiation and the inlet and ambient temperature values of the HTF. In this graph, the line equation for thermal efficiency exhibits a decreasing slope. Although the efficiency of the system is relatively low, it complies with the ASHRAE 93-863 standard for thermal applications [46-49].

## 5. Conclusion

In this collector with a compact area of 15 m<sup>2</sup>, temperatures of around 120–140 °C were obtained (Fig. 5). The theoretical thermal power is around 5 kW, and the experimental thermal power is around 4 kW (Fig. 7).

Flat mirrors, which are similar to those used in Fresnel collectors, were employed in this experimental set. These 11 cm-wide flat mirrors were mounted on a parabolic surface, which resembles the configuration in Fresnel collectors. Considering that flat mirrors were placed on the parabolic surface, some of the rays escape from the focal center. Consequently, the thermal and optical efficiency of this collector is lower than that of collectors using one-piece mirrors [36]. However, given the difficulty in acquiring parabolic monolithic mirrors in the market, they remain a favorable choice due to their ease of manufacture. The heights and gaps between the mirrors should be minimized to enhance thermal efficiency. Similar to other studies, Arun worked on a hybrid system by placing flat mirrors on a parabolic surface as in Fresnel collectors. He found that the overall thermal efficiency in this hybrid system reached 39 %

[34]. In the current experimental study, the theoretical thermal efficiency of the system was found to be around 55 %, and the experimental thermal efficiency during the day was found to be approximately 30 %–39 % (Fig. 6).

## Acknowledgments

This collector was manufactured with the facilities of GAPYENEV (GAP Renewable Energy and Energy Efficiency Center), which was established in Şanlıurfa to popularize the use of renewable energy resources in the Southeastern Anatolia Region, Turkey.

## References

- [1] A. Z. Hafez et al., Design analysis of solar parabolic trough thermal collectors, *Renewable and Sustainable Energy Reviews*, 82 (2018) 1215-1260.
- [2] S. A. Kalogirou, *Solar Energy Engineering Processes and Systems*, Second Edition, Elsevier, The Netherlands (2014).
- [3] Z. Said, Energy, exergy, economic and environmental (4E) analysis of a parabolic trough solar collector using MXene based silicone oil nanofluids, *Solar Energy Materials and Solar Cells*, 239 (2022) 111633.
- [4] K. Mohammad, Techno-economic analysis and environmental benefits of solar industrial process heating based on parabolic trough collectors, *Sustainable Energy Technologies and Assessments*, 47 (2021) 101412.
- [5] A. Kumar, A review on exergy analysis of solar parabolic collectors, *Solar Energy*, 197 (2020) 411-432.
- [6] E. Bellos and C. Tzivanidis, Iterative designs of parabolic trough solar collectors, *Progress in Energy and Combustion Science*, 71 (2019) 81-117.
- [7] T. U. Shinde et al., Thermal performance analysis of novel receiver for parabolic trough solar collector, *Energy*, 254 (2022) 124343.
- [8] E. Anabela et al., A review of the use of nanofluids as heat-transfer fluids in parabolic-trough collectors, *Applied Thermal Engineering*, 211 (2022) 118346.
- [9] E. Guimar Barbosa et al., Experimental evaluation of a stationary parabolic trough solar collector: influence of the concentrator and heat transfer fluid, *Journal of Cleaner Production*, 276 (2020) 124174.
- [10] I. Eleazar et al., Design and construction of a parabolic trough solar collector for process heat production, *Energy Procedia*, 57 (2014) 2149-2158.
- [11] P. V. Gharat, Chronological development of innovations in reflector systems of parabolic trough solar collector (PTC) - A review, *Renewable and Sustainable Energy Reviews*, 145 (2021) 111002.
- [12] O. A. Begdouri and A. El Fadar, Impact of parabolic trough collector model on the CSP plants' performance, *New Journal and We have not Received Input Yet*, 34 (2022) 101434.
- [13] R. Pal and K. Ravi Kumar, Investigations of thermo-hydrodynamics, structural stability, and thermal energy storage

- for direct steam generation in parabolic trough solar collector: A comprehensive review, *Journal of Cleaner Production*, 311 (2021) 127550.
- [14] A. Y. Al-Rabeeah, Experimental investigation of improved parabolic trough solar collector thermal efficiency using novel receiver geometry design, *International Journal of Thermofluids*, 18 (2023) 100344.
- [15] M. Uzair, N. ur Rehman and S. A. Raza, Probabilistic approach for estimating heat fluid exit temperature correlation in a linear parabolic trough solar collector, *Journal of Mechanical Science and Technology*, 32 (2018) 447-453.
- [16] N. U. Uzair Rehman and M. Asif, Optical design of a novel polygonal trough collector for solar concentrating photovoltaic applications, *Arabian Journal for Science and Engineering*, 46 (2021) 2963-2973.
- [17] A. Goe et al., Inspection of dynamic modelling and control of a parabolic trough solar collector, *Materialstoday: Proceedings*, 80 (Part 1) (2023) 92-97.
- [18] K. D. Ramesh and K. Suresh, Thermal performance of parabolic trough collector with absorber tube misalignment and slope error, *Solar Energy*, 184 (2019) 249-259.
- [19] J. Platzer Werner, Linear fresnel collector (LFC) solar thermal technology, K. Lovegrove and W. Stein (Ed.), *Woodhead Publishing Series in Energy, Concentrating Solar Power Technology*, Second Edition, Woodhead Publishing (2021) 165-217.
- [20] E. Batuecas, Environmental and energetic behavior of a beam-down linear Fresnel solar field for low-grade thermal energy applications, *Applied Thermal Engineering*, 231 (2023) 121002.
- [21] M. Montes et al., Performance model and thermal comparison of different alternatives for the Fresnel single-tube receiver, *Applied Thermal Engineering*, 104 (2016) 162-175.
- [22] E. Bellos et al., Experimental and numerical investigation of a linear Fresnel solar collector with flat plate receiver, *Energy Conversion and Management*, 130 (2016) 44-59.
- [23] G. Morin et al., Comparison of linear Fresnel and parabolic trough collector power plants, *Solar Energy*, 86 (2012) 1-12.
- [24] G. Zhu, T. Wendelin, M. J. Wagner and C. Kutscher, History, current state, and future of linear fresnel concentrating solar collectors, *Solar Energy*, 103 (2014) 639-652.
- [25] P. L. Singh, R. M. Sarviya and J. L. Bhagoria, Thermal performance of linear Fresnel reflecting solar concentrator with trapezoidal cavity absorbers, *Applied Energy*, 87 (2010) 541-550.
- [26] Z. Yanqing et al., Design and experimental investigation of a stretched parabolic linear Fresnel reflector collecting system, *Energy Conversion and Management*, 126 (2016) 89-98.
- [27] E. Bellos et al., Experimental investigation of the daily performance of an integrated linear Fresnel reflector system, *Solar Energy*, 167 (2018) 220-230.
- [28] Z. Hongfei et al., Design and experimental analysis of a cylindrical compound Fresnel solar concentrator, *Solar Energy*, 107 (2014) 26-37.
- [29] A. Rawani, S. P. Sharma, K. D. P. Singh and K. Namarata, Analytical modeling of parabolic linear collectors for solar power plant, *Journal of Mechanical Science and Technology*, 32 (10) (2018) 4993-5004.
- [30] J. Ma, Optimized design of a linear Fresnel collector with a compound parabolic secondary reflector, *Renewable Energy*, 171 (2021) 141-148.
- [31] N. Kincaid, An optical performance comparison of three concentrating solar power collector designs in linear Fresnel, parabolic trough, and central receiver, *Applied Energy*, 231 (2018) 1109-1121.
- [32] P. Lal Singh, Thermal performance of linear Fresnel reflecting solar concentrator with trapezoidal cavity absorbers, *Applied Energy*, 87 (2010) 541-550.
- [33] A. Jaber Abdulhamed, Review of solar parabolic-trough collector geometrical and thermal analyses, performance, and applications, *Renewable and Sustainable Energy Reviews*, 91 (2018) 822-831.
- [34] N. D. Kaushika, Performance of a low cost solar paraboloidal dish steam generating system, *Energy Conversion and Management*, 41 (2000) 713-726.
- [35] C. Çetiner, Experimental and theoretical analyses of a double-cylindrical trough solar concentrator, *Journal of Mechanical Science and Technology*, 34 (2020) 4857-4863.
- [36] A. Kumar Ramasamy, Design and performance investigation of modified hybrid parabolic linear fresnel collector, *Energy for Sustainable Development*, 76 (2023) 101273.
- [37] G. Morin, Comparison of linear fresnel and parabolic trough collector power plants, *Solar Energy*, 86 (1) (2012) 1-12.
- [38] M. J. Montes et al., A comparative analysis of configurations of linear Fresnel collectors for concentrating solar power, *Energy*, 73 (2014) 192-203.
- [39] J. A. Duffie and W. A. Beckman, *Solar Energy Thermal Processes*, John Wiley and Sons, New York, USA (1991).
- [40] A. Kılıç, *Solar Energy*, Kipaş Distributorship (1984).
- [41] F. P. Incropera and D. P. DeWitt, *Heat and Mass Transfer*, Literatür Publishing, Istanbul (2001).
- [42] J. S. Hesieh, *Solar Energy Engineering*, Prentice-Hall, USA (1986).
- [43] M. Allam, Heat transfer enhancement in parabolic trough receivers using inserts: A review, *Energy for Sustainable Development*, 76 (2023) 101273.
- [44] N. Eskin, Transient performance analysis of cylindrical parabolic concentrating collectors and comparison with experimental results, *Energy Conversion and Management*, 40 (1999) 175-191.
- [45] J. Satpute, Thermal performance investigation of concentrated solar collector using novel aluminum absorber, *Materials Today: Proceedings*, 5 (2018) 4059-4065.
- [46] H. B. Kulkarni, Design, and development of prototype cylindrical parabolic solar collector for water heating application, *International Journal of Renewable Energy Development*, 5 (1) (2016) 49-55.
- [47] O. Helal, B. Chaouachi and S. Gabsi, Design and thermal performance of an ICS solar water heater based on three parabolic sections, *Solar Energy*, 85 (2011) 2421-2432.
- [48] J. K. Nayak, E. Y. Amer and S. M. Deshpande, Comparison

of three transient methods for testing solar flat-plate collector, *Energy Conversions and Management*, 4 (2000) 677-700.

- [49] E. Venegas-Reyes et al., Design, construction, and testing of a parabolic trough solar concentrator for hot water and low enthalpy steam generation, *Journal of Renewable and Sustainable Energy*, 4 (2012) 53-103.



**Cuma Çetiner** completed his Ph.D. He received his Ph.D. degree from Sakarya University in Turkey. He works as an Assistant Professor at Harran University. His research interests include solar energy and renewable energy.